

Study on Fluorescence Recognition of CrO_4^{2-} and $\text{Cr}_2\text{O}_7^{2-}$ Based on Zn-MOF

Xiwen Xing*, Han Wang

College of Chemistry and Chemical Engineering, China University of Petroleum (East China),
Qingdao, China, 266580

* Corresponding Author Email: 18343004349@163.com

Abstract. In contemporary society, as industrialization and urbanization advance rapidly, the problem of chromium-containing wastewater discharge has grown increasingly conspicuous. Hexavalent chromium salts (CrO_4^{2-} and $\text{Cr}_2\text{O}_7^{2-}$), as common heavy metal ions, pose a severe threat to both the environment and human health. Therefore, the progress of efficient and sensitive detection technologies is crucial for monitoring such environmental pollutants. In this study, 2,6-naphthalenedicarboxylic acid and 4,7-bis(4-pyridyl) benzothiadiazole were employed as ligands to synthesize a zinc-based metal-organic framework (MOF-1) through a solvothermal approach. The successful preparation of the MOF-1 was verified through powder X-ray diffraction (PXRD) analysis. MOF-1 exhibits specific recognition capabilities for CrO_4^{2-} and $\text{Cr}_2\text{O}_7^{2-}$ through the mechanism of fluorescence quenching. Interference experiments, conducted using $\text{Cr}_2\text{O}_7^{2-}$ as a representative anion, confirmed that MOF-1 can accurately identify $\text{Cr}_2\text{O}_7^{2-}$ even in the presence of other coexisting anions, demonstrating excellent selectivity. Titration experiments revealed that the fluorescence intensity of MOF-1 diminishes as the concentrations of CrO_4^{2-} and $\text{Cr}_2\text{O}_7^{2-}$ increase, showing a typical concentration-dependent quenching behavior. The quenching constants (K_{sv}) were determined to be $1.96 \times 10^4 \text{ M}^{-1}$ and $2.68 \times 10^4 \text{ M}^{-1}$ for CrO_4^{2-} and $\text{Cr}_2\text{O}_7^{2-}$, respectively, indicating high sensitivity. This sensing mechanism is attributed to the significant spectral overlap between the ultraviolet absorption spectra of $\text{CrO}_4^{2-}/\text{Cr}_2\text{O}_7^{2-}$ and the excitation spectrum of MOF-1. The competitive absorption of excitation energy by these ions reduces the energy available for MOF-1, thereby decreasing its fluorescence intensity. The combination of high sensitivity and selectivity highlights the significant advantages of MOF-1 as a fluorescent sensing agent for hexavalent ion detection, providing reliable technical support for environmental monitoring and analytical testing applications.

Keywords: Luminescence sensor; Metal-organic frameworks; CrO_4^{2-} and $\text{Cr}_2\text{O}_7^{2-}$.

1. Introduction

As the global population keeps growing, environmental pollution has become increasingly severe, with water pollution emerging as a particularly critical issue. Among various pollutants, chromium-containing wastewater has attracted widespread societal attention due to its high toxicity and carcinogenicity, making the development of effective treatment and detection methods an urgent need [1]. Hexavalent chromium, as a key chemical reagent, is widely utilized in industrial processes such as metal surface treatment, leather processing, and dye/pigment manufacturing. Its unique chemical properties and reactivity contribute significantly to enhancing production efficiency and product quality [1]. However, residual hexavalent chromium oxyanions (e. g., $\text{Cr}_2\text{O}_7^{2-}$ and CrO_4^{2-}) in industrial wastewater pose severe hazards, exhibiting acute toxicity as well as carcinogenic and mutagenic potential, thus presenting substantial threats to both the environment and human health. Consequently, there is an urgent need for reliable detection and remediation strategies [1]. To this point, various fluorescent probes have been created for the detection of these hazardous analytes., including "silver quantum dots (QDs)" [2], "carbon dots (CDs)" [3], "conjugated microporous polymers (CMPs)" [4], "metal-organic frameworks (MOFs)" [5] [6], "inorganic nanomaterials" [7], and "small-molecule fluorescent sensors" [8]. Among these, metal-organic frameworks (MOFs) have garnered increasing research interest due to their unique advantages, such as tunable pore sizes, facile

surface modification, and high specific surface area. These structurally innovative MOFs not only expand the diversity of metal-organic framework architectures but also demonstrate remarkable application potential in fluorescence analysis—particularly in the detection of $\text{Cr}_2\text{O}_7^{2-}$ and CrO_4^{2-} ions, where MOFs exhibit outstanding performance.

This study represents the first application of a dual-ligand combination of 2,6-naphthalenedicarboxylic acid and 4,7-bis(4-pyridinyl)benzothiadiazole for the recognition and detection of CrO_4^{2-} and $\text{Cr}_2\text{O}_7^{2-}$ ions. Experimental results show that the material exhibits superior recognition performance for target ions compared to previously reported studies in the same field. Moreover, we have probed into its recognition mechanism, confirming that it functions through competitive absorption induced by the overlap between its excitation spectrum and the aviolet absorption of target ions, and this in turn results in fluorescence quenching. During this process, the material's structure remains stable without significant signal fluctuations. Furthermore, MOF-1 can accurately identify target ions even in complex matrices, displaying excellent anti-interference capability and thus offering a new approach for the efficient detection of hexavalent chromium.

2. Experimental Procedures

2.1. Materials and methods

All chemical reagents were commercially purchased. Fourier transform infrared (FT-IR) spectra were recorded on a Nicolet 5700 FT-IR spectrometer. Powder X-ray diffraction (PXRD) patterns were collected using a Bruker D8 Advanced diffractometer. Luminescent sensing experiments were performed on a Hitachi F-7000 spectrometer. UV-visible absorption spectra were measured with a UH4150 spectrophotometer.

2.2. Preparation of MOF-1

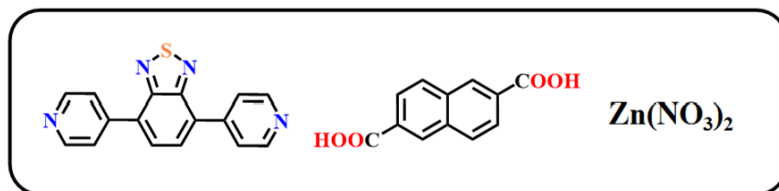


Figure 1. The organic ligands used for preparation MOF-1.

The synthesis process of MOF-1 is as follows: 0.05 mmol of $\text{Zn}(\text{NO}_3)_2 \cdot 6\text{H}_2\text{O}$, 0.02 mmol of 2,6-naphthalenedicarboxylic acid (2,6-NDA), 0.01 mmol of 4,7-di(4-pyridinyl)-2,1,3-benzothiadiazole (DPBT), 1 mL N, N-dimethylformamide (DMF), and 1.5 mL H_2O are added to a reactor lined with 20 mL polytetrafluoroethylene. The mixture is sonicated at room temperature for 15 minutes to ensure thorough mixing and uniform dispersion. The reactor was then heated to 100°C and subjected to a solvothermal reaction for 11 hours, followed by cooling to 45°C and filtration to obtain light yellow needle-like crystals. After washing with water and drying, MOF-1 was obtained. Figure 1 shows the synthesized MOF-1.

To verify the successful synthesis of MOF-1, the product was characterized using X-ray powder diffraction (PXRD). As shown in Figure 2, the peak positions in the PXRD pattern of the prepared MOF-1 match those of the single-crystal crystal simulation reported in the literature, indicating that the synthesized product has good crystallinity and purity, laying a solid foundation for subsequent experiments [9].

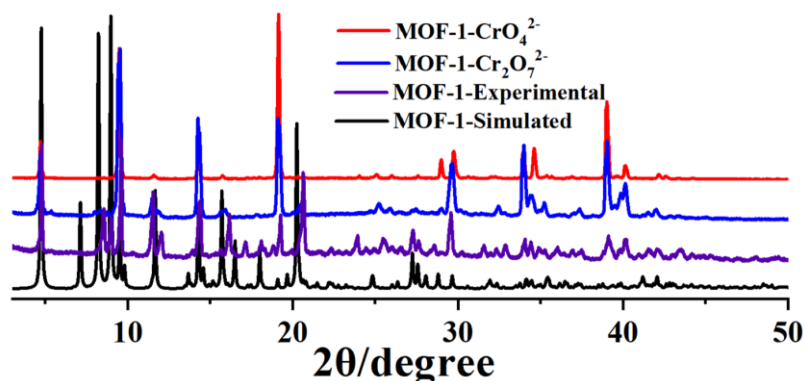


Figure 2. The simulated PXRD and the Experimental PXRD of MOF-1 and the PXRD patterns of MOF-1 after immersed in $\text{Cr}_2\text{O}_7^{2-}$ and CrO_4^{2-} .

2.3. Fluorescence detection experiment

Grind the MOF-1 material into a fine powder. Take 2 mg of this powder and disperse it evenly in 2 mL of H_2O . Then, use an ultrasonic device to treat the mixture for 30 minutes to ensure that the MOF powder is fully dispersed in the aqueous solution. During this process, corresponding analytes can be added to the solution according to the specific needs and objectives of the experiment for further analysis or experimental operations.

3. Results and Discussion

3.1. Photoluminescence properties

To thoroughly investigate the fluorescence characteristics of MOF-1, water was used as the dispersing medium. Figure 3 provides a detailed display of the excitation and emission peak spectra of MOF-1, which shows an emission peak at 451 nm when excited at a wavelength (λ_{ex}) of 358 nm.

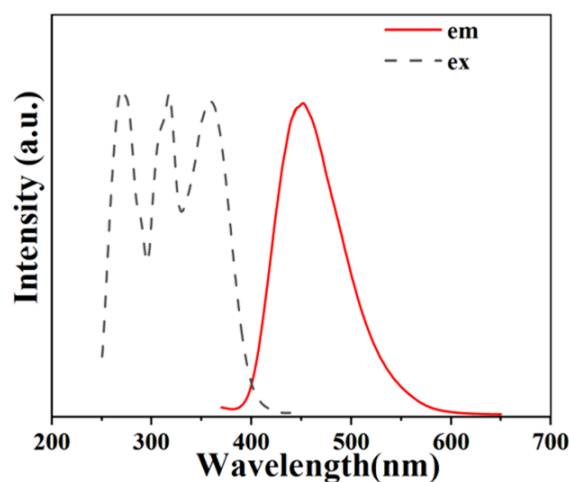


Figure 3. The excitation and emission of MOF-1 in H_2O .

3.2. Detection of CrO_4^{2-} and $\text{Cr}_2\text{O}_7^{2-}$

The misuse of hexavalent chromium ions (e. g. CrO_4^{2-} and $\text{Cr}_2\text{O}_7^{2-}$) causes severe ecological pollution, highlighting the urgency of developing specific metal-organic frameworks (MOFs) for their identification. In this study, MOF-1 was evaluated as a fluorescent sensor through a series of selectivity experiments using various potassium salts to verify its detection performance. Specifically, MOF-1 was exposed to solutions containing Br^- , $\text{C}_2\text{O}_4^{2-}$, Cl^- , CO_3^{2-} , $\text{Cr}_2\text{O}_7^{2-}$, F^- , H_2PO_4^- , I^- , NO_3^- , PO_4^{3-} , and CrO_4^{2-} to investigate its fluorescence recognition capabilities [10]. As illustrated in Figure 4a, significant fluorescence quenching of MOF-1 was only observed in the presence of CrO_4^{2-} and $\text{Cr}_2\text{O}_7^{2-}$, indicating that the material exhibits excellent selective recognition for these two chromate

ions. To further validate its performance in complex environments, anti-interference experiments were conducted using $\text{Cr}_2\text{O}_7^{2-}$ as a model analyte. As shown in Figure 4b, MOF-1 maintained robust recognition performance for $\text{Cr}_2\text{O}_7^{2-}$ even when coexisting with other ions. These results confirm that the proposed method possesses high anti-interference capability, enabling accurate identification of target $\text{Cr}_2\text{O}_7^{2-}$ in multi-component systems. Consequently, this method holds substantial practical value for real-world applications, particularly in scenarios requiring the selective detection of specific analytes within complex matrices.

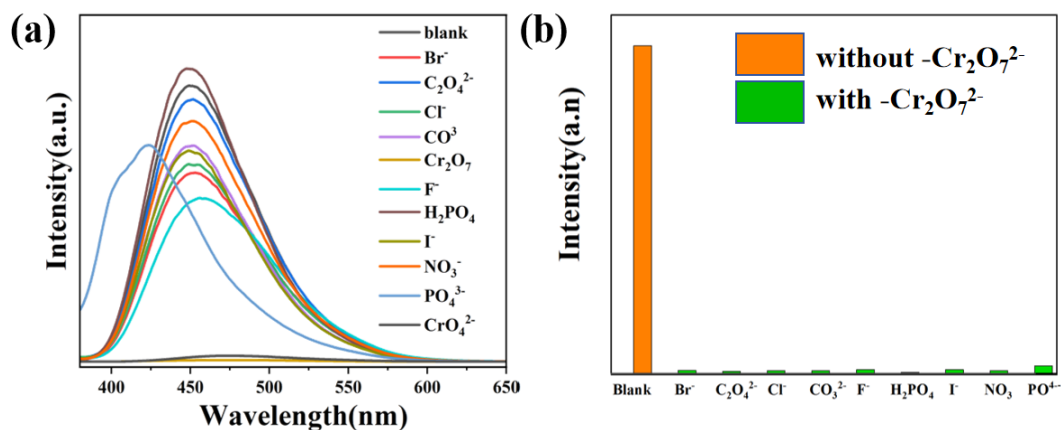


Figure 4. (a) The emission spectra of MOF-1 in aqueous solutions with different anions. (b) Comparative analysis of MOF-1's fluorescence intensities in the presence of $\text{Cr}_2\text{O}_7^{2-}$.

Then quantitative experiments were made to examine the correlation between fluorescence intensity and concentrations of CrO_4^{2-} and $\text{Cr}_2\text{O}_7^{2-}$, respectively. From 5a, as CrO_4^{2-} solution with concentration ranging from 0 to 30mM was added gradually into MOF suspension, fluorescence emission intensity of MOF-1 at wavelength of 450nm reduced gradually as well following a concentration dependent quenching behavior. On the contrary, Figure 5b indicates the quenching effect of $\text{Cr}_2\text{O}_7^{2-}$ on MOF-1 fluorescence which is in lower concentration range (0 - 0.15 mM). An increase in the concentration of CrO_4^{2-} is accompanied by a decrease in fluorescence intensity, as the quenching becomes more prominent. To investigate the Fluorescent response of the MOF to the hexavalent chromium ions, we used the Stern-Volmer (SV) equation ($I_0/I = 1 + K_{sv}[M]$, where I_0/I is the emitted intensity of MOF-1 of the solution before and after addition of $\text{Cr}_2\text{O}_7^{2-}$ or CrO_4^{2-} , $[M]$ is the concentration of $\text{Cr}_2\text{O}_7^{2-}$ or CrO_4^{2-} , and K_{sv} is the fluorescence quenching) to the Fluorescence response data [11]. Within the low concentration range, the fluorescence quenching curves of both CrO_4^{2-} and $\text{Cr}_2\text{O}_7^{2-}$ conformed to this classical equation. Figures 5c and 5d display the Stern-Volmer fitting results for the two ions, respectively, with experimental data showing good agreement with the theoretical model, thereby validating the reliability of the recognition mechanism. For CrO_4^{2-} detection, the linear correlation coefficient (R^2) was 0.994, and the quenching constant (K_{sv}) reached $1.96 \times 10^4 \text{ M}^{-1}$. For $\text{Cr}_2\text{O}_7^{2-}$, a higher quenching efficiency was observed, with a K_{sv} value of $2.68 \times 10^4 \text{ M}^{-1}$ and a linear correlation coefficient (R^2) of 0.977. These experiments demonstrate that the MOF sensor exhibits excellent detection performance for hexavalent chromium ions, providing a highly sensitive fluorescent sensing platform for the accurate and quantitative detection of chromium pollution in aquatic environments. Table 1 lists the quenching constants (K_{sv}) for the detection of $\text{Cr}_2\text{O}_7^{2-}$, CrO_4^{2-} by other reported methods. The comparative results show that MOF-1 exhibits superior sensitivity in the detection of $\text{Cr}_2\text{O}_7^{2-}$, CrO_4^{2-} compared with other materials.

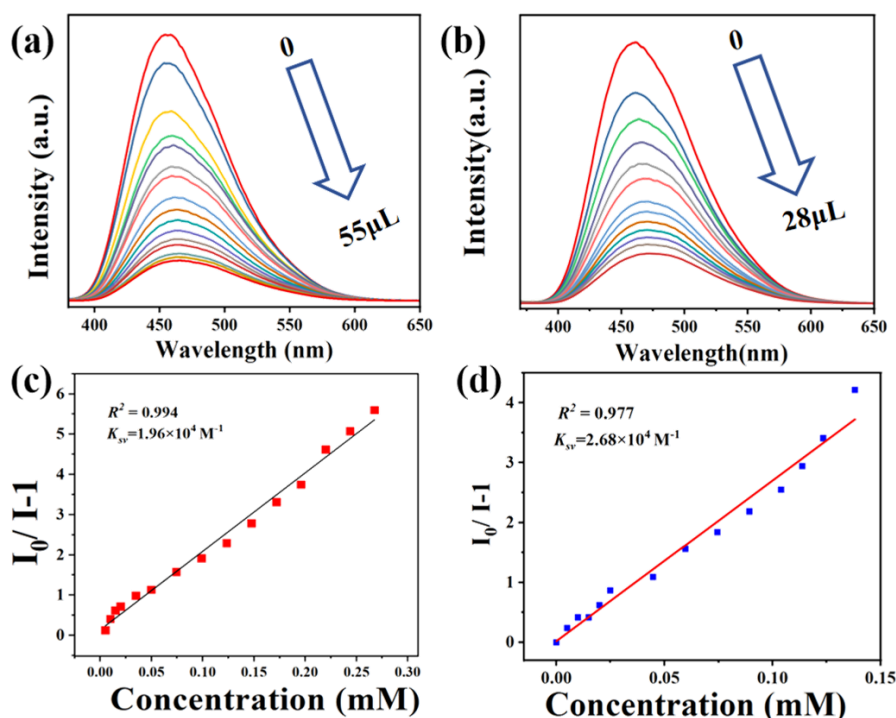


Figure 5. Sensitive experiments of MOF-1 towards CrO_4^{2-} (a), $\text{Cr}_2\text{O}_7^{2-}$ (b). S-V graph of MOF-1 for CrO_4^{2-} (c), $\text{Cr}_2\text{O}_7^{2-}$ (d).

Table 1. Comparison of MOF-1 with other MOFs

| Name | $\text{Cr}_2\text{O}_7^{2-}\text{-K}_{sv}$ | $\text{CrO}_4^{2-}\text{-K}_{sv}$ | Reference |
|---|--|-----------------------------------|-----------|
| $\{[(\text{CH}_3)_2\text{NH}_2]_2[\text{Zn}_5(\text{TDA})_4(\text{TZ})_4] \cdot 4\text{DMF}\}_n$ | $6.77 \times 10^3 \text{ M}^{-1}$ | $5.84 \times 10^3 \text{ M}^{-1}$ | [12] |
| $\text{Eu}^{3+} @ \{[(\text{CH}_3)_2\text{NH}_2]_2[\text{Zn}_5(\text{TDA})_4(\text{TZ})_4] \cdot 4\text{DMF}\}_n$ | $9.98 \times 10^3 \text{ M}^{-1}$ | $1.13 \times 10^4 \text{ M}^{-1}$ | [12] |
| $[\text{Y}(\text{BTC})(\text{H}_2\text{O})_6]_n : 0.1\text{Eu}$ | $4.52 \times 10^3 \text{ M}^{-1}$ | $1.18 \times 10^3 \text{ M}^{-1}$ | [13] |
| $[\text{Zn}(\text{btz})]_n$ | $4.23 \times 10^3 \text{ M}^{-1}$ | $1.19 \times 10^3 \text{ M}^{-1}$ | [14] |
| $[\text{Eu}(\text{L}1)(\text{HCOO})(\text{H}_2\text{O})]_n$ | $2.76 \times 10^3 \text{ M}^{-1}$ | $1.54 \times 10^3 \text{ M}^{-1}$ | [15] |
| $[(\text{CH}_3)_2\text{NH}_2][\text{Eu}_4(\text{FDA})_7(\text{DMF})_2]$ | $1.25 \times 10^4 \text{ M}^{-1}$ | $3.56 \times 10^3 \text{ M}^{-1}$ | [16] |
| $\text{Eu} @ \text{Zr-MOF}$ | $6.746 \times 10^4 \text{ M}^{-1}$ | Not described | [17] |
| MOF-1 | $2.68 \times 10^4 \text{ M}^{-1}$ | $1.96 \times 10^4 \text{ M}^{-1}$ | This work |

3.3. Fluorescence quenching mechanism

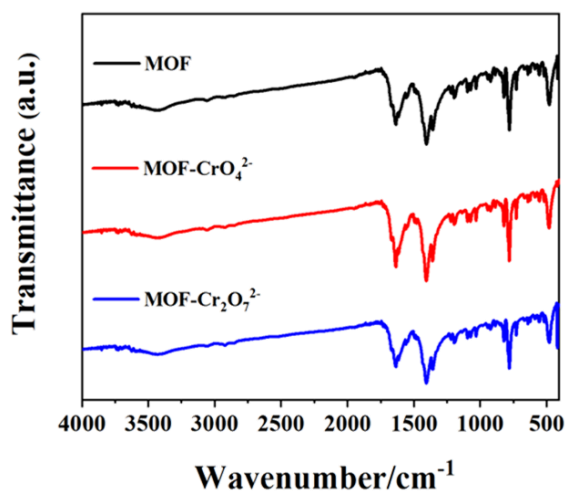


Figure 6. IR of MOF-1 before and after immersed in $\text{Cr}_2\text{O}_7^{2-}$ and CrO_4^{2-} .

First, the MOF materials were separately immersed in aqueous solutions of $\text{Cr}_2\text{O}_7^{2-}$ and CrO_4^{2-} , yielding MOF-1- $\text{Cr}_2\text{O}_7^{2-}$ and MOF-1- CrO_4^{2-} . To rule out the possibility of MOF-1 fluorescence quenching caused by framework collapse, PXRD testing was first conducted on MOF-1- $\text{Cr}_2\text{O}_7^{2-}$ and MOF-1- CrO_4^{2-} . The test results showed that the characteristic peak positions of MOF-1, MOF-1- $\text{Cr}_2\text{O}_7^{2-}$, and MOF-1- CrO_4^{2-} were consistent, indicating that the MOF-1 structure remained intact and ruling out the possibility of fluorescence quenching due to framework collapse. Subsequently, FT-IR spectroscopy tests were conducted. The characteristic absorption peak positions of MOF-1 before and after immersion in $\text{Cr}_2\text{O}_7^{2-}$ and CrO_4^{2-} showed no significant shift, and no new coordination characteristic peaks appeared, confirming that MOF-1 did not coordinate with $\text{Cr}_2\text{O}_7^{2-}$ or CrO_4^{2-} (Figure 6). The combined results of PXRD and FT-IR indicate that the MOF-1 framework remains intact and no coordination occurs.

The primary mechanisms underlying fluorescence quenching between MOF-1 and the analyte are Förster Resonance Energy Transfer (FRET) and Competitive Absorption (CA). For FRET to occur, two conditions must be met: first, the emission spectrum of MOF-1 must overlap with the ultraviolet absorption spectrum of the target ion, and second, the interaction distance between the two must be less than 10 nm. The occurrence of the FRET mechanism is closely related to spectral overlap: when the emission spectrum of MOF-1 overlaps with the UV absorption spectrum of the analyte, and the interaction distance between the two is less than 10 nm, the excited state of MOF-1 transfers energy to the analyte through dipole-dipole interactions, thereby causing its own fluorescence quenching [1]. In contrast, for the competitive absorption (CA) mechanism to operate, there must be an overlap between the excitation spectrum of MOF-1 and the UV absorption spectrum of the analyte. In this case, the analyte competitively captures the excited energy: When the UV absorption spectrum of the analyte overlaps with the excitation spectrum of MOF-1, the competitive absorption (CA) mechanism comes into play. Specifically, energy competition arises within the excitation wavelength range due to overlapping absorption spectra. After the analyte absorbs part of the excitation energy, the excitation energy obtained by MOF-1 decreases, thereby hindering its energy-dependent fluorescence transition, ultimately resulting in fluorescence quenching [18]. In summary, when combined with Figure 7, the absorption spectra of $\text{Cr}_2\text{O}_7^{2-}$ and CrO_4^{2-} exhibit a considerable degree of congruence with the excitation spectrum of MOF-1, yet there is virtually no overlap with the emission spectrum of MOF-1. This result indicates that in this system, the primary mechanism of fluorescence quenching is CA, where $\text{Cr}_2\text{O}_7^{2-}$ and CrO_4^{2-} competitively absorb excitation energy, leading to MOF-1 fluorescence quenching, rather than the FRET mechanism.

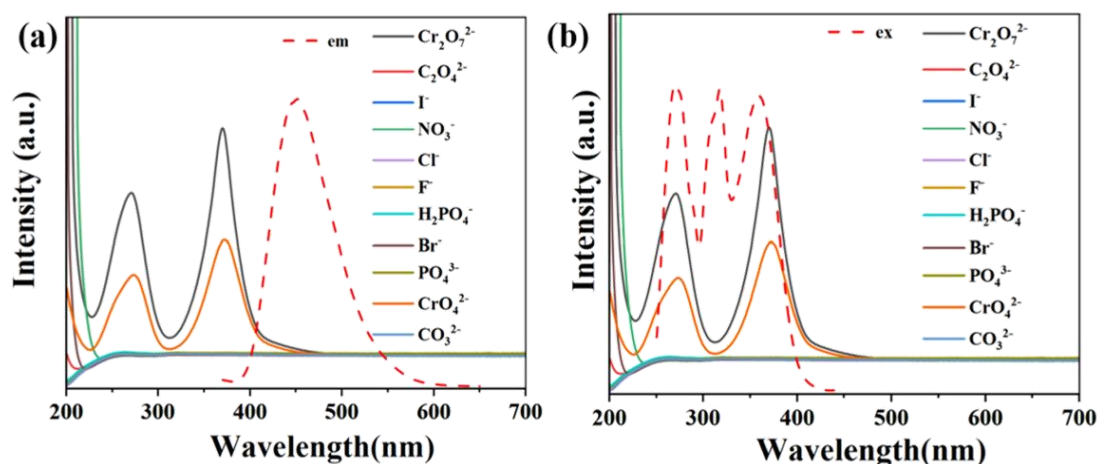


Figure 7. (a) The intersection of the analyte's UV-vis absorption spectrum with the emission spectrum of MOF-1. (b) The intersection of the analyte's UV-vis absorption spectrum with the excitation spectrum of MOF-1.

4. Conclusion

This study synthesized MOF-1 using 2,6-naphthalenedicarboxylic acid and 4,7-bis(4-pyridinyl)benzothiadiazole as ligands via a solvothermal method, with its structure confirmed by PXRD. The material exhibits unique fluorescent properties in water and can selectively recognize CrO_4^{2-} and $\text{Cr}_2\text{O}_7^{2-}$ through fluorescence quenching, maintaining good selectivity even in the presence of coexisting anions. Titration tests revealed the fluorescence intensity of the material decreases with an increase in the concentration of target ions. Utilizing the Stern-Volmer equation, the K_{sv} value for CrO_4^{2-} is $1.96 \times 10^4 \text{ M}^{-1}$ ($R^2=0.994$) and that for $\text{Cr}_2\text{O}_7^{2-}$ is $2.68 \times 10^4 \text{ M}^{-1}$ ($R^2=0.977$), with sensitivity superior to most reported MOF materials. Mechanistic analysis revealed that the fluorescence quenching originates from competitive absorption (CA), and the framework structure of MOF-1 remains stable without new coordination interactions after the reaction. This study provides MOF-based fluorescent sensing technical support for the environmental monitoring of hexavalent chromium in chromium-containing wastewater. In the future, the team will optimize the synthesis process to improve yield and reduce costs; explore functional modifications to enhance compatibility with portable detection devices; develop on-site identification devices for hexavalent chromium, regulate ligand structures, and expand the detection capability for various pollutants, laying a foundation for comprehensive water quality analysis. In the long term, it is expected to promote the development of practical environmental monitoring technologies and provide more reliable solutions for water safety management.

References

- [1] Li W, Liao G, Wang C. Synergistically electronic interacted PVDF/CdS/TiO₂ organic-inorganic photocatalytic membrane for multi-field driven panel wastewater purification [J]. *Applied Catalysis B: Environmental*, 2024, 344: 123484.
- [2] L. A. Al-Khateeb, M. El-Maghrabey, R. El-Shaheny, Sensitive determination of naftazone using carbon quantum dots nanoprobe by fluorimetry and smartphone-based techniques, *Spectrochim. Acta, Part A* 302 (2023) 123109.
- [3] Y. Wang, F. Zhang, J. Liu, B. Yang, Y. Yuan, Y. Zhou, et al., A fluorescence nanoprobe of N-Acetyl-L-Cysteine capped CdTe QDs for sensitive detection of nitrofurazone, *Spectrochim. Acta, Part A* 297 (2023) 122709.
- [4] C. Qi, H. Liu, J. Lyu, H. Zhao, Z. Y. Lu, Anthracene and porphyrin-based conjugated microporous polymer for nitrofurazone antibiotics and nitroaromatic explosives. detection, *J. Environ. Chem. Eng.* 11 (2023) 111553.
- [5] Z. Zhao, H. Gong, X. Wang, Y. Liu, Z. Pan, Y. Wang, et al., A fluorescent Zinc-based coordination polymer for sensing antibiotic pollutants, *Inorg. Chem. Commun* 155 (2023) 111078.
- [6] R. Singhaal, N. A. Ashashi, C. Sen, S. Devi, H. N. Sheikh, Fabrication of dual functional 3D-flower shaped NaYF₄: Dy³⁺/Eu³⁺ and graphene oxide based NaYF₄: Dy³⁺/Eu³⁺ nanocomposite material as a potable luminescence sensor and photocatalyst for environmental pharmaceutical pollutant nitrofurazone in aquatic medium, *Nano-Struct. Nano-Objects* 34 (2023) 100965.
- [7] R. Zheng, K. Zhang, Dual-emission Sm (III)-macrocyclic as the lab-on-a-molecule chemosensor for nitroaromatic antibiotic analogues, *Polyhedron* 245 (2023) 116635.
- [8] T. Verma, P. Verma, U. P. Singh, A multi responsive phosphonic acid based fluorescent sensor for sensing Fe³⁺, benzaldehyde and antibiotics, *Microchem. J.* 191 (2023) 108771.
- [9] Ru J, Shi Y X, Yang Q Y, Li T, Wang H Y, Cao F, Guo Q, Wang Y L. A benzothiadiazole-based Zn (II) metal-organic framework with visual turn-on sensing for anthrax biomarker and theoretical calculation [J]. *Molecules*, 2024, 29 (12): 2755.
- [10] Song L J. Construction of Functional Fluorescent MOFs Materials and Their Sensing Performance for Biomarkers [D]. Hohhot: Inner Mongolia University, 2021.
- [11] Zhang, R. J., Wang, J. J., Xu, H., Zhu, Z. H., Zheng, T. F., Peng, Y., Chen, J. L., Liu, S. J., Wen, H. R. Stable Cd(II)-Based Metal-Organic Framework as a Multiresponsive Luminescent Sensor for Acetylacetone, Salicylaldehyde, and Benzaldehyde with High Sensitivity and Selectivity. *Cryst. Growth Des.* 2023, 23, 5564.
- [12] Gui W J, Du M Z, Zhang X M, Almási M, Wan L J, Gan L, Wang Z X, Wu S H. A strategy to obtain highly luminescent MOF-76 based on hydrothermal annealing treatment [J]. *Journal of Alloys and Compounds*, 2022, 919: 165881.
- [13] Qin B., Zhang X., Qiu J., et al. (2021). *Inorganic Chemistry*, 60 (3), 1716 - 1725.

- [14] Li J., Zhang H., Wang, Y. (2023). One cadmium (II)-based metal–organic framework as high-efficiency multi-functional fluorescence chemosensor targeting for the determination of Fe^{3+} , $\text{Cr}_2\text{O}_7^{2-}$ and CrO_4^{2-} in aqueous phase. *Journal of Hazardous Materials*, 452, 131245.
- [15] Riedel, Z. W., Pearson Jr., D. R., Karigerasi, M. H., Soares, J. A. N. T., Goldschmidt, E. A., Shoemaker, D. P (2022). Synthesis of $\text{Eu}(\text{HCOO})_3$ and $\text{Eu}(\text{HCOO})_3 \cdot (\text{HCONH}_2)_2$ crystals and observation of their $^5\text{D}_0 \rightarrow ^7\text{F}_0$ transition for quantum information systems. arXiv preprint arXiv: 2203.04487.
- [16] X. Wang, X. Zhang, Y. Li, X. Zhao (2017). Multi-Responsive Luminescent Sensors Based on Two-Dimensional Lanthanide–Metal Organic Frameworks for Highly Selective and Sensitive Detection of Cr (III) and Cr (VI) Ions and Benzaldehyde. *Crystal Growth & Design*, 17 (8), 4410 - 4417.
- [17] X. Zhang ,Y. Li, X. Wang, et al. Eu^{3+} -anchoring Zirconium-organic framework for enhancing fluorescence sensing detection sensitivity towards Cr (VI) ions [J]. *Journal of Molecular Structure*, 2023, 1284: 135407.
- [18] J. R. Lakowicz. *Principles of Fluorescence Spectroscopy* [M]. 3rd ed. New York: Springer, 2006: XXI - 954.